Int. J. Electron. Commun. (AEÜ) 139 (2021) 153909

Contents lists available at ScienceDirect

Int. J. Electron. Commun. (AEÜ)

journal homepage: www.elsevier.com/locate/aeue

Regular paper

Combining RF energy harvesting and cooperative communications for low-power wide-area systems

Xuan Nam Tran [a], Van-Phuc Hoang [a,*], Ba Cao Nguyen [b]

[a] Le Quy Don Technical University, Ha Noi, Viet Nam
[b] Telecommunications University, Khanh Hoa, Viet Nam

ARTICLE INFO

Keywords:
Low-power wide-area network
Long range
Energy harvesting
Cooperative communication
Outage probability
Throughput
Symbol error probability

ABSTRACT

This paper presents the combination of energy harvesting (EH) at the wireless sensor and cooperative communications for low-power wide-area (LPWA) systems. Firstly, the Internet of Things sensor harvests the energy from the power beacon with multiple transmit antennas via radio frequency signals and then uses the harvested energy to transmit signals to multiple gateways with multiple receive antennas. Then, the cooperative communications is applied at the server based on the gateway outputs. By mathematical analysis, we derive the exact closed-form expressions of outage probabilities (OPs), throughput, and symbol error probabilities (SEPs) of the EH-LPWA system over Nakagami-*m* fading channel in the cases without and with cooperative communications. Our expressions can be considered as the first results applying EH for LPWA systems with mathematical analysis. Then, we obtain the optimal value of the time switching ratio that minimizes the OPs and SEPs and maximizes the throughput of the considered EH-LPWA system. Numerical results have clarified that, the distances, path loss exponent, and data transmission rate have a strong impact on the OPs, throughput, and SEPs. Particularly, using a half of transmission blocks for EH can maximize the system performance. Moreover, when the number of transmit antennas at power beacon is equal to the number of receive antennas at gateways, the system performance can be improved significantly. Finally, the accuracy of the obtained expressions is demonstrated via Monte-Carlo simulations.

1. Introduction

Recently, energy harvesting (EH) from radio frequency (RF) signals has been widely used to satisfy the energy requirements of wireless communication systems. Hence, it becomes a promising forthcoming technique to be deployed in the fifth generation (5G) and beyond networks [1,2]. Specifically, EH can supply enough power for sensor in Internet of things (IoT) systems, heterogeneous networks (HetNets), mobile devices, and extremely remote area communications. In addition, wireless devices can transmit the RF signals over the air for a long range, thus, EH from RF signals can be applied for many devices that are located in the restricted areas, where the traditional energy grid is extremely difficult to be deployed. For example, RF EH power supply is very promising for IoT based smart environment monitoring systems with energy efficient Beat sensors and LoRaWAN communications [3]. Consequently, the researches and experiments about EH are developed quickly so that we could apply this technique for the current and future wireless systems soon [4–6].

In the literature, the linear and non-linear energy harvesters have been proposed to apply the EH technique for wireless devices [1,7]. In particular, the wireless devices can harvest the energy from base stations [8–10] or power beacons [11]. The mathematical analysis was used to derive the expressions in terms of outage probability (OP), throughput, and symbol error probability (SEP) of the EH communication systems [8,11]. It was shown that for a certain EH system, there is an optimal value of the time switching ratio which can minimize the system OP/SEP. Also, using multiple antennas for the power beacon can greatly improve the performance of EH systems because of a significant increase about the amount of harvested energy. In addition, the non-linear characteristics of energy harvesters cause the power ceiling for the harvested energy leading to a error floor of OP/SEP in EH system [12]. Furthermore, EH technique is combined with various new techniques such as full-duplex (FD), cognitive radio (CR), spatial modulation (SM), and non-orthogonal multiple access (NOMA) for enhancements in both energy and spectral efficiencies [8,11–14]. In addition to the mathematical analysis, the experimental measurements were also used to investigate the amount of harvested energy and the performance of EH communication systems in practice [7,15,16].

* Corresponding author.
E-mail addresses: namtx@lqdtu.edu.vn (X.N. Tran), phuchv@lqdtu.edu.vn (V.-P. Hoang), nguyenbacao@tcu.edu.vn (B.C. Nguyen).

https://doi.org/10.1016/j.aeue.2021.153909
Received 17 April 2021; Accepted 23 July 2021
Available online 27 July 2021

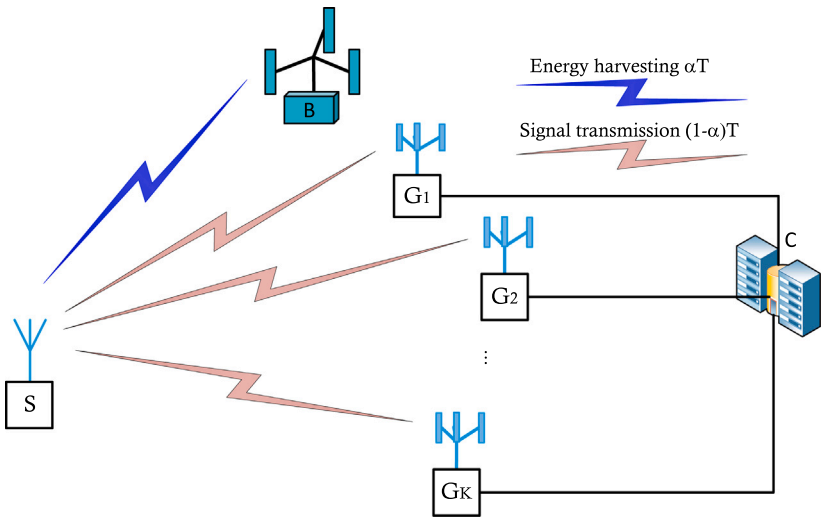

Fig. 1. Illustration of the considered EH-LPWA system.

On the other hand, the current wireless communication systems such as Long-term Evolution (LTE) and WiFi are usually designed for short-range networks so that these systems can achieve reliable communications and high speed data transmissions [17]. However, the disadvantages of these systems are the high energy consumption and the high deployment cost. Meanwhile, other systems such as ZigBee and Bluetooth can consume the low power but these systems also operate for a short-range with the low speed [18,19]. Consequently, these systems are not suitable for LoRaWAN communications because of the low power consumption requirement of LoRaWAN systems. In this context, low-power wide-area (LPWA) network technologies have been emerged as the promising connectivity solutions for IoT devices in recent years due to their advantages [17,20]. Particularly, LPWA technologies can reduce the power consumption with the low delay sensitivity and wide coverage. Therefore, LPWA systems can solve various issues in the current wireless communication networks such as battery life, deployment cost, and coverage [17,18,21,22]. The recent reports observed that, LPWA systems are highly promising for IoT requirements. Specifically, the LoRaWAN is a physical layer technology developed by Semtech, where an adaptive data rate chirp modulation technology is used to allow the flexible long-range communications with the low design cost and low power consumption [18,21,23]. Consequently, the LPWA system range depends on the transmission power, coding scheme, and data rate [23]. To provide the robustness performance of the LPWA systems, a type of the chirp spread spectrum with the integrated forward error correction is often used. Also, a special chirp spread spectrum technique can be used in a bidirectional communications [18].

Beside the applications of LPWA systems for IoT devices, the performance of LPWA systems has been also investigated in the literature. In [22], a disruptive approach was proposed to increase the number of users used in LoRaWAN systems. By applying time-power multiplexing, the network capacity was significantly improved because the gateways can transmit more-than-one packets at the same time. Similarly [22], the works in [21] considered LoRaWAN networks with an increase of IoT devices. The uplink OP was investigated over Poisson distributed channels when the interferences between IoT devices were taken into account. It was shown that the OP was greatly impacted by the interferences, distances, and the number of IoT devices. In [24], a theoretical analysis is conducted to investigate the feasibility of the transmission of a LoRa wide-area system via various conditions such as the effects of spreading factor (SF) and heights of transmit antennas. Their test results indicated that the system can transmit and receive at a long distance of 8.33 km. Together with the measured experiments, the mathematical analysis of LPWA systems was firstly performed in [25]. Specifically, [25] derived the OP and bit error rate (BER) expressions of LPWA systems and validated them via computer simulations.

As the above discussions, both EH and LPWA network technologies have many advantages and can be applied for various applications in IoT systems. Also, the benefits of EH technique have been discussed and experimented to clarify the potentials of this technique when being deployed in the LPWA systems [20,26]. However, the combination of the EH technique and LPWA technology have not been applied in the literature in terms of the mathematical analysis. Meanwhile, this combination is very important due to the fact that EH from RF signals has great potentials to supply the stable energy to low power energy-constrained systems such as wireless sensor networks, IoTs, and extremely remote area communications used in 5G and beyond networks [1,2]. In particular, the amount of harvested energy can fully satisfy the power requirements of IoT devices in LPWA systems. Therefore, exploiting EH technique for LPWA systems is inevitable in the future. This observation motivates us to consider an EH-LPWA system where the IoT sensors can harvest the energy from power beacon and then use the harvested energy for transmitting signals. By using the mathematical analysis, we obtain the exact closed-from expressions of OPs, throughputs, and SEPs of the considered EH-LPWA system. So far, this is the first work that mathematically analyzes the performance of LPWA systems with EH technique. The main contributions of the paper are summarized as follows:

- We investigate an EH-LPWA system where EH technique is exploited. Specifically, the IoT sensor is located in a restricted area, where the traditional power grid is extremely difficult to be deployed. Thus, it has to harvest the energy from the power beacon before transmitting signals to gateways. In addition, power beacon and gateways are equipped with multiple antennas.
- We obtain the exact closed-form expressions of OPs, throughputs, and SEPs of the considered EH-LPWA system over Nakagami-m fading channels for both cases without and with cooperative communications. Then, we derive the optimal value of the time switching ratio that minimizes the OPs and SEPs and maximizes the throughput of the considered EH-LPWA system. Due to the generic properties of the Nakagami-m fading channels, we can easily derive the OPs, throughputs, and SEPs of the considered EH-LPWA system over other channels such as Gaussian, Rayleigh, and Rician channels by changing the value of m. We validate all derived expressions through Monte-Carlo simulations.
- We evaluate the performance of the considered EH-LPWA system for various scenarios. Particularly, the numerical analysis results

clarify that the data transmission rates, the distances, the time switching ratio for EH, the number of transmit/receive antennas, and the Nakagami parameters greatly impact on the OPs, throughputs, and SEPs of the system. By using a half of transmission block for EH, the system performance can be optimized. When the total of transmit and receive antennas are constant, we can use the number of transmit antennas at PB equal to the number of receive antennas at gateways to achieve the lowest OP/SEP of the considered EH-LPWA system.

The rest of this paper is organized as follows. Section 2 presents the system and signal models of the considered EH-LPWA system without and with cooperative communication. Section 3 analyzes the system performance by mathematically deriving the OP and SEP expressions for both cases without and with cooperative communication. Section 4 provides the detail calculatiions to obtain the optimal value of the time switching ratio. Section 5 provides numerical results and discussions. Finally, Section 6 concludes this paper.

2. System model

The considered EH-LPWA system is illustrated in Fig. 1. The system consists of a power beacon (B), an IoT sensor (S), K gateways ($G_1, G_2, \ldots, G_K$), and a server center (C). Specifically, S has only one antenna while B and G_k ($k = 1, 2, \ldots, K$), respectively, have M and N antennas. Since B and G_k are equipped with multiple antennas, there are parallel transmissions in the considered EH-LPWA system, i.e., the EH channels (from B to S) and the information channels (from S to G_k). It is also noted that multi-antenna configurations are often used in cellular technologies, however, these configurations can be used in the LPWA systems to satisfy the requirements of connectivity to massive number of devices distributed in the large geographical areas at an unprecedented low-cost [17,18,20]. In addition, S is located in a restricted area, it is difficult to supply power to it. Therefore, S has to harvest the energy from B via radio frequency (RF) signals for data transmission.[1] Noticing that in the case of we cannot deploy the power beacon for transmitting the energy via RF signals, S can harvest the energy from gateways. This is similar to that the relay harvests the energy from source or base station in cellular network [5,6]. However, the transmission power of gateways is often lower than that of the power beacon. Meanwhile, the considered EH-LPWA system is applied for long range transmission. Thus, the harvested energy from gateways may not be enough for transmitting signals from S to gateways successfully. Therefore, the power beacon is chosen in our work to enhance the harvested energy at S. Since EH from RF signals can provide stable energy to IoT devices used in 5G and B5G networks [1,7], the considered EH-LPWA system can be deployed in various applications including the traffic management, health care systems, environmental monitoring, and smart buildings [27–30].

As presented in the literature, there are two common EH schemes, e.g., time switching (TS) and power splitting (PS), often used for EH wireless systems. Particularly, in the low data transmission rates, the TS scheme can achieve higher OP and throughput performance than those of PS scheme [31]. However, PS scheme is better than TS scheme for high data transmission rates. Due to the fact that the LPWA systems often operate in low data transmission rates [18], the performance in terms of OP, throughput, and SEP of the considered EH-LPWA system can be better than that with TS scheme. As a result, we use TS scheme for considering the system performance. There are two stages corresponding to TS scheme for the system operation, as shown in Fig. 2. Firstly, S harvests the energy from B using the interval αT, where α is the time switching ratio satisfying $0 \le \alpha \le 1$ and T is the transmission block. Secondly, S transmits signals to all gateways using the remain interval $(1-\alpha)T$. Since the energy harvester at S is configured for harvesting the energy via RF signals transmitted from B, other signals such as noise term is filtered by the RF circuits of the energy harvester [32]. In other words, the energy harvester at S only receives the RF signal from B for harvesting the energy.

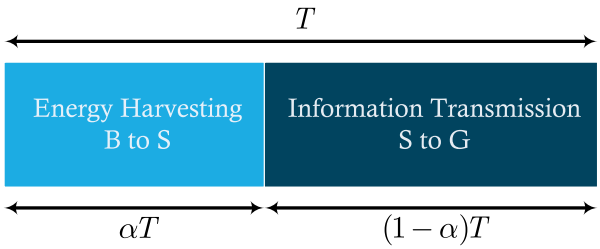

Fig. 2. TS protocol for the considered EH-LPWA system.

In the interval of EH, the harvested energy at S (denoted by E_S) is given as

$$E_S = \frac{\eta \alpha T P_B d_{BS}^{-\beta} \|\mathbf{h}_{BS}\|^2}{M}, \tag{1}$$

where η is the energy conversion efficiency ($0 \le \eta \le 1$); P_B is the total transmission power of B; d_{BS} is the distance between B and S; $2 \le \beta \le 6$ is the path-loss exponent; $\mathbf{h}_{BS}$ is the channel vector from M transmit antennas of B to one receive antenna of S.[2] Then, the harvested energy at S is transformed to the supply power for signal transmission. The transmit power of S is thus given as

$$P_S = \frac{E_S}{(1-\alpha)T} = \frac{\eta \alpha T P_B d_{BS}^{-\beta} \|\mathbf{h}_{BS}\|^2}{M(1-\alpha)T} = \frac{\eta \alpha P_B \|\mathbf{h}_{BS}\|^2}{M(1-\alpha) d_{BS}^{\beta}}. \tag{2}$$

The received signals at G_k in the interval $(1-\alpha)T$ is computed as

$$y_{G_k} = \mathbf{h}_{SG_k} \sqrt{P_S d_{SG_k}^{-\beta}}\, x_S + z_{G_k}, \tag{3}$$

where $\mathbf{h}_{SG_k}$ is the channel vector from one transmit antenna of S to N receive antennas of the kth gateway; x_S is the transmitted signal at S; d_{SG_k} is the distance from S to the kth gateway; z_{G_k} is the Gaussian noise at the kth gateway with zero mean and the variance of σ^2, i.e., $z_{G_k} \sim \mathcal{CN}(0, \sigma^2)$.

At each gateway, maximum ratio combining (MRC) is applied to maximize the received signal power. Consequently, the signal-to-noise

[1] Since EH from RF signals is often used for a short range, the distance between B and S may be short, not long as the LPWA system requirements. Therefore, we can use a suitable frequency for B–S channel to satisfy the requirements about the transmission ranges of the considered EH-LPWA systems. In the case that high frequencies (i.e., frequencies used in 5G or 6G systems) have to be used in the considered systems, including the B–S channel, we can locate B in a convenient location where B–S channel is available to provide the supply power to S via RF signals. On the other hand, in the case that the environment has high path loss exponent, it is necessary to apply various methods such as orthogonal frequency division multiplexing and channel coding for improving the system performance.

[2] It is worth noticing that the energy harvester in practice is often nonlinear, thus, the output power of the energy harvester depend on a saturation power threshold P_{th}. In particular, when the input power is higher than P_{th}, the output power is still unchanged. There are various factors such as diode and saturation nonlinearities causing the nonlinear features of the energy harvester [1,10]. Furthermore, it is difficult to avoid the saturation nonlinearities of energy harvesting circuits in realistic systems. Consequently, the harvested energy at S with nonlinear energy harvester can be derived by extending (1) as

$$E_S = \begin{cases} \frac{\eta \alpha T d_{BS}^{-\beta} P_B \|\mathbf{h}_{BS}\|^2}{M}, & P_B \|\mathbf{h}_{BS}\|^2 \le P_{th}, \\ \frac{\eta \alpha T d_{BS}^{-\beta} P_{th}}{M}, & P_B \|\mathbf{h}_{BS}\|^2 > P_{th}. \end{cases}$$

(SNR) ratio at the kth gateway is calculated as

$$\gamma_{\mathrm{G}_k} = \frac{\|\mathbf{h}_{\mathrm{SG}_k}\|^2 P_{\mathrm{S}} d_{\mathrm{SG}_k}^{-\beta}}{\sigma^2}. \tag{4}$$

In the case of cooperative communications, the distances from S to all gateways are normalized for combining the signal at the server center [25]. Thus, the received signal at C is now expressed as

$$y_{\mathrm{C}} = \sqrt{P_{\mathrm{S}} \sum_{k=1}^{K} \|\mathbf{h}_{\mathrm{SG}_k}\|^2 d_0^{-\beta}}\, x_{\mathrm{S}} + z_{\mathrm{C}}, \tag{5}$$

where $d_0 = \min(d_{\mathrm{SG}_1}, d_{\mathrm{SG}_2}, \ldots, d_{\mathrm{SG}_K})$, and z_{C} is the Gaussian noise term.

From (5), the SNR at C is computed as

$$\gamma_{\mathrm{C}} = \frac{P_{\mathrm{S}} \sum_{k=1}^{K} \|\mathbf{h}_{\mathrm{SG}_k}\|^2 d_0^{-\beta}}{\sigma^2}. \tag{6}$$

Replacing P_{S} from (2) into (4) and (6), the SNR at the kth gateway and C are, respectively, expressed as

$$\gamma_{\mathrm{G}_k} = \frac{\eta\alpha P_{\mathrm{B}} \|\mathbf{h}_{\mathrm{BS}}\|^2 \|\mathbf{h}_{\mathrm{SG}_k}\|^2}{M\sigma^2(1-\alpha) d_{\mathrm{BS}}^{\beta} d_{\mathrm{SG}_k}^{\beta}}, \tag{7}$$

$$\gamma_{\mathrm{C}} = \frac{\eta\alpha P_{\mathrm{B}} \|\mathbf{h}_{\mathrm{BS}}\|^2 \sum_{k=1}^{K} \|\mathbf{h}_{\mathrm{SG}_k}\|^2}{M\sigma^2(1-\alpha) d_{\mathrm{BS}}^{\beta} d_0^{\beta}}. \tag{8}$$

3. Performance analysis

3.1. Outage probability

The OP of the considered EH-LPWA system is defined as the probability when the instantaneous data transmission rate is lower than the pre-defined data transmission rate. Mathematically, the OPs in the cases without and with cooperative communications are, respectively, computed as

$$\mathcal{P}_k = \Pr\Big\{(1-\alpha)\log_2(1+\gamma_{\mathrm{G}_k}) < \mathcal{R}\Big\}, \tag{9}$$

$$\mathcal{P}_{\mathrm{C}} = \Pr\Big\{(1-\alpha)\log_2(1+\gamma_{\mathrm{C}}) < \mathcal{R}\Big\}, \tag{10}$$

where γ_{G_k} and γ_{C} are, respectively, given in (7) and (8); $\mathcal{R}$ is the pre-defined data transmission rate. It should be noted that, the pre-defined data transmission rate is calculated as the number of bits transmitted over the air per second via a bandwidth of 1 Hz. In other words, the pre-defined data transmission rate is also called as the spectral efficiency (bit/s/Hz) when the bandwidth is normalized as 1 Hz.

Let $\gamma_{\mathrm{th}} = 2^{\frac{\mathcal{R}}{1-\alpha}} - 1$ be the outage threshold, (9) and (10) can be rewritten as

$$\mathcal{P}_k = \Pr\Big\{\gamma_{\mathrm{G}_k} < \gamma_{\mathrm{th}}\Big\}, \tag{11}$$

$$\mathcal{P}_{\mathrm{C}} = \Pr\Big\{\gamma_{\mathrm{C}} < \gamma_{\mathrm{th}}\Big\}. \tag{12}$$

From (11) and (12), the OPs of the considered system are derived by the following Theorem 1.

Theorem 1. *The OPs of the considered EH-LPWA system with energy harvesting in the cases without and with cooperative communications over Nakagami-m fading channel are given as*

$$\mathcal{P}_k = 1 - \frac{2}{\Gamma(m_k N)} \left(\frac{m_k}{\Omega_k}\right)^{m_k N} \sum_{i=0}^{m_s M-1} \frac{1}{i!} \left(\frac{m_s M\sigma^2(1-\alpha) d_{\mathrm{BS}}^{\beta} d_{\mathrm{SG}_k}^{\beta} \gamma_{\mathrm{th}}}{\Omega_s \eta\alpha P_{\mathrm{B}}}\right)^{i} \times \left(\frac{\Omega_k m_s M\sigma^2(1-\alpha) d_{\mathrm{BS}}^{\beta} d_{\mathrm{SG}_k}^{\beta} \gamma_{\mathrm{th}}}{\Omega_s m_k \eta\alpha P_{\mathrm{B}}}\right)^{\frac{m_k N-i}{2}} \times \mathcal{K}_{m_k N-i}\left(2\sqrt{\frac{m_s m_k M\sigma^2(1-\alpha) d_{\mathrm{BS}}^{\beta} d_{\mathrm{SG}_k}^{\beta} \gamma_{\mathrm{th}}}{\Omega_s \Omega_k \eta\alpha P_{\mathrm{B}}}}\right), \tag{13}$$

$$\mathcal{P}_{\mathrm{C}} = 1 - \frac{2}{\Gamma(m_k K N)} \left(\frac{m_k}{\Omega_k}\right)^{m_k K N} \sum_{i=0}^{m_s M-1} \frac{1}{i!} \left(\frac{m_s M\sigma^2(1-\alpha) d_{\mathrm{BS}}^{\beta} d_0^{\beta} \gamma_{\mathrm{th}}}{\Omega_s \eta\alpha P_{\mathrm{B}}}\right)^{i} \times \left(\frac{\Omega_k m_s M\sigma^2(1-\alpha) d_{\mathrm{BS}}^{\beta} d_0^{\beta} \gamma_{\mathrm{th}}}{\Omega_s m_k \eta\alpha P_{\mathrm{B}}}\right)^{\frac{m_k K N-i}{2}} \times \mathcal{K}_{m_k K N-i}\left(2\sqrt{\frac{m_s m_k M\sigma^2(1-\alpha) d_{\mathrm{BS}}^{\beta} d_0^{\beta} \gamma_{\mathrm{th}}}{\Omega_s \Omega_k \eta\alpha P_{\mathrm{B}}}}\right), \tag{14}$$

where m_s, m_k and Ω_s, Ω_k denote the Nakagami parameters and the average channel gains of B–S and S–G_k channels, respectively; $\Gamma(.)$ is the gamma function; $\mathcal{K}_{m_k N-i}(.)$ and $\mathcal{K}_{m_k K N-i}(.)$ are the $m_k N - i$ and $m_k K N - i$ order modified Bessel functions of the second kind [33], respectively.

Proof. Replacing γ_{G_k} and γ_{C} in (7) and (8) into (11) and (12), respectively, the OPs are now expressed as

$$\begin{aligned}\mathcal{P}_k &= \Pr\left\{\frac{\eta\alpha P_{\mathrm{B}} \|\mathbf{h}_{\mathrm{BS}}\|^2 \|\mathbf{h}_{\mathrm{SG}_k}\|^2}{M\sigma^2(1-\alpha) d_{\mathrm{BS}}^{\beta} d_{\mathrm{SG}_k}^{\beta}} < \gamma_{\mathrm{th}}\right\} \\ &= \Pr\left\{\|\mathbf{h}_{\mathrm{BS}}\|^2 \|\mathbf{h}_{\mathrm{SG}_k}\|^2 < \frac{M\sigma^2(1-\alpha) d_{\mathrm{BS}}^{\beta} d_{\mathrm{SG}_k}^{\beta} \gamma_{\mathrm{th}}}{\eta\alpha P_{\mathrm{B}}}\right\} \\ &= 1 - \int_0^{\infty} \left[1 - F_{\|\mathbf{h}_{\mathrm{BS}}\|^2}\left(\frac{M\sigma^2(1-\alpha) d_{\mathrm{BS}}^{\beta} d_{\mathrm{SG}_k}^{\beta} \gamma_{\mathrm{th}}}{\eta\alpha P_{\mathrm{B}} y}\right)\right] f_{\|\mathbf{h}_{\mathrm{SG}_k}\|^2}(y) dy,\end{aligned} \tag{15}$$

$$\begin{aligned}\mathcal{P}_{\mathrm{C}} &= \Pr\left\{\frac{\eta\alpha P_{\mathrm{B}} \|\mathbf{h}_{\mathrm{BS}}\|^2 \sum_{k=1}^{K} \|\mathbf{h}_{\mathrm{SG}_k}\|^2}{M\sigma^2(1-\alpha) d_{\mathrm{BS}}^{\beta} d_0^{\beta}} < \gamma_{\mathrm{th}}\right\} \\ &= \Pr\left\{\|\mathbf{h}_{\mathrm{BS}}\|^2 \sum_{k=1}^{K} \|\mathbf{h}_{\mathrm{SG}_k}\|^2 < \frac{M\sigma^2(1-\alpha) d_{\mathrm{BS}}^{\beta} d_0^{\beta} \gamma_{\mathrm{th}}}{\eta\alpha P_{\mathrm{B}}}\right\} \\ &= 1 - \int_0^{\infty} \left[1 - F_{\|\mathbf{h}_{\mathrm{BS}}\|^2}\left(\frac{M\sigma^2(1-\alpha) d_{\mathrm{BS}}^{\beta} d_0^{\beta} \gamma_{\mathrm{th}}}{\eta\alpha P_{\mathrm{B}} z}\right)\right] f_{\sum_{k=1}^{K} \|\mathbf{h}_{\mathrm{SG}_k}\|^2}(z) dz,\end{aligned} \tag{16}$$

where $F(.)$ and $f(.)$ are the cumulative distribution function (CDF) and the probability density function (PDF) of the instantaneous channel gain amplitude, respectively.

To derive the exact closed-form expressions from (15) and (16), firstly, we obtain the CDF and PDF of the instantaneous channel gain following Nakagami-m distribution. For only one channel gain, i.e., $|h|^2$, the CDF and PDF are, respectively, given as

$$\begin{aligned}F_{|h|^2}(x) &= \frac{1}{\Gamma(m)} \gamma\left(m, \frac{mx}{\Omega}\right) \\ &= 1 - \exp\left(-\frac{mx}{\Omega}\right) \sum_{i=0}^{m-1} \frac{1}{i!} \left(\frac{mx}{\Omega}\right)^{i}, \; x \geq 0,\end{aligned} \tag{17}$$

$$f_{|h|^2}(x) = \left(\frac{m}{\Omega}\right)^{m} \frac{x^{m-1}}{\Gamma(m)} \exp\left(-\frac{mx}{\Omega}\right), \; x \geq 0, \tag{18}$$

where $\gamma(.,.)$ is the lower incomplete gamma function; m and Ω are, respectively, the Nakagami parameter and the average channel gain of $|h|^2$.

When maximal-ratio-transmission (MRT) and maximal-ratio-combining (MRC) techniques are applied at the transmitter/receiver, such as MRT at power beacon and MRC at kth gateway or the server center, the CDF and PDF of channel gains, i.e, $\|\mathbf{h}_{\mathrm{BS}}\|^2$ are expressed as [34]:

$$F_{\|\mathbf{h}_{\mathrm{BS}}\|^2}(x) = 1 - \exp\left(-\frac{m_s x}{\Omega_s}\right) \sum_{i=0}^{m_s M-1} \frac{1}{i!} \left(\frac{m_s x}{\Omega_s}\right)^{i}, \quad x \geq 0, \tag{19}$$

$$f_{\|\mathbf{h}_{\mathrm{BS}}\|^2}(x)=\left(\frac{m_s}{\Omega_s}\right)^{m_sM}\frac{x^{m_sM-1}}{\Gamma(m_sM)}\exp\left(-\frac{m_sx}{\Omega_s}\right),\ x\geq 0. \tag{20}$$

Now, applying (19) and (20), the probabilities in (15) and (16) are solved as

$$\begin{aligned}\mathcal{P}_k=&1-\int_0^{\infty}\exp\left(-\frac{m_sM\sigma^2(1-\alpha)d_{\mathrm{BS}}^{\beta}d_{\mathrm{SG}_k}^{\beta}\gamma_{\mathrm{th}}}{\Omega_s\eta\alpha P_{\mathrm{B}}y}\right)\\&\times\sum_{i=0}^{m_sM-1}\frac{1}{i!}\left(\frac{m_sM\sigma^2(1-\alpha)d_{\mathrm{BS}}^{\beta}d_{\mathrm{SG}_k}^{\beta}\gamma_{\mathrm{th}}}{\Omega_s\eta\alpha P_{\mathrm{B}}y}\right)^i\\&\times\left(\frac{m_k}{\Omega_k}\right)^{m_kN}\frac{y^{m_kN-1}}{\Gamma(m_kN)}\exp\left(-\frac{m_ky}{\Omega_k}\right)dy\\=&1-\frac{1}{\Gamma(m_kN)}\left(\frac{m_k}{\Omega_k}\right)^{m_kN}\sum_{i=0}^{m_sM-1}\frac{1}{i!}\left(\frac{m_sM\sigma^2(1-\alpha)d_{\mathrm{BS}}^{\beta}d_{\mathrm{SG}_k}^{\beta}\gamma_{\mathrm{th}}}{\Omega_s\eta\alpha P_{\mathrm{B}}}\right)^i\\&\times\int_0^{\infty}y^{m_kN-i-1}\exp\left(-\frac{m_sM\sigma^2(1-\alpha)d_{\mathrm{BS}}^{\beta}d_{\mathrm{SG}_k}^{\beta}\gamma_{\mathrm{th}}}{\Omega_s\eta\alpha P_{\mathrm{B}}y}-\frac{m_ky}{\Omega_k}\right)dy,\end{aligned} \tag{21}$$

$$\begin{aligned}\mathcal{P}_{\mathrm{C}}=&1-\int_0^{\infty}\exp\left(-\frac{m_sM\sigma^2(1-\alpha)d_{\mathrm{BS}}^{\beta}d_0^{\beta}\gamma_{\mathrm{th}}}{\Omega_s\eta\alpha P_{\mathrm{B}}z}\right)\\&\times\sum_{i=0}^{m_sM-1}\frac{1}{i!}\left(\frac{m_sM\sigma^2(1-\alpha)d_{\mathrm{BS}}^{\beta}d_0^{\beta}\gamma_{\mathrm{th}}}{\Omega_s\eta\alpha P_{\mathrm{B}}z}\right)^i\\&\times\left(\frac{m_k}{\Omega_k}\right)^{m_kKN}\frac{z^{m_kKN-1}}{\Gamma(m_kKN)}\exp\left(-\frac{m_kz}{\Omega_k}\right)dz\\=&1-\frac{1}{\Gamma(m_kKN)}\left(\frac{m_k}{\Omega_k}\right)^{m_kKN}\sum_{i=0}^{m_sM-1}\frac{1}{i!}\left(\frac{m_sM\sigma^2(1-\alpha)d_{\mathrm{BS}}^{\beta}d_0^{\beta}\gamma_{\mathrm{th}}}{\Omega_s\eta\alpha P_{\mathrm{B}}}\right)^i\\&\times\int_0^{\infty}z^{m_kKN-i-1}\exp\left(-\frac{m_sM\sigma^2(1-\alpha)d_{\mathrm{BS}}^{\beta}d_0^{\beta}\gamma_{\mathrm{th}}}{\Omega_s\eta\alpha P_{\mathrm{B}}z}-\frac{m_kz}{\Omega_k}\right)dz.\end{aligned} \tag{22}$$

Applying [33, Eq. (3.471.9)], two above integrals are computed as

$$\begin{aligned}&\int_0^{\infty}y^{m_kN-i-1}\exp\left(-\frac{m_sM\sigma^2(1-\alpha)d_{\mathrm{BS}}^{\beta}d_{\mathrm{SG}_k}^{\beta}\gamma_{\mathrm{th}}}{\Omega_s\eta\alpha P_{\mathrm{B}}y}-\frac{m_ky}{\Omega_k}\right)dy\\&=2\left(\frac{\Omega_km_sM\sigma^2(1-\alpha)d_{\mathrm{BS}}^{\beta}d_{\mathrm{SG}_k}^{\beta}\gamma_{\mathrm{th}}}{\Omega_sm_k\eta\alpha P_{\mathrm{B}}}\right)^{\frac{m_kN-i}{2}}\\&\times\mathcal{K}_{m_kN-i}\left(2\sqrt{\frac{m_sm_kM\sigma^2(1-\alpha)d_{\mathrm{BS}}^{\beta}d_{\mathrm{SG}_k}^{\beta}\gamma_{\mathrm{th}}}{\Omega_s\Omega_k\eta\alpha P_{\mathrm{B}}}}\right),\end{aligned} \tag{23}$$

$$\begin{aligned}&\int_0^{\infty}z^{m_kKN-i-1}\exp\left(-\frac{m_sM\sigma^2(1-\alpha)d_{\mathrm{BS}}^{\beta}d_0^{\beta}\gamma_{\mathrm{th}}}{\Omega_s\eta\alpha P_{\mathrm{B}}z}-\frac{m_kz}{\Omega_k}\right)dz\\&=2\left(\frac{\Omega_km_sM\sigma^2(1-\alpha)d_{\mathrm{BS}}^{\beta}d_0^{\beta}\gamma_{\mathrm{th}}}{\Omega_sm_k\eta\alpha P_{\mathrm{B}}}\right)^{\frac{m_kKN-i}{2}}\\&\times\mathcal{K}_{m_kKN-i}\left(2\sqrt{\frac{m_sm_kM\sigma^2(1-\alpha)d_{\mathrm{BS}}^{\beta}d_0^{\beta}\gamma_{\mathrm{th}}}{\Omega_s\Omega_k\eta\alpha P_{\mathrm{B}}}}\right).\end{aligned} \tag{24}$$

Replacing (23) and (24) into (21) and (22), respectively, we obtain the exact closed-form expressions of OPs of the considered EH-LPWA system in Theorem 1. Hence, the proof is completed.

3.2. Symbol error probability

The SEP of the considered EH-LPWA system is expressed as

$$\mathrm{SEP}=a\mathbb{E}\{Q(\sqrt{b\gamma})\}=\frac{a}{\sqrt{2\pi}}\int_0^{\infty}F\left(\frac{t^2}{b}\right)e^{-\frac{t^2}{2}}dt, \tag{25}$$

where (a,b) is a couple of the modulation types, i.e., $(a,b)=(1,2)$ and $(a,b)=(2,1)$ for the binary phase-shift keying (BPSK) and 4-quadrature amplitude modulation (4-QAM), respectively [35]. Other values of (a,b) are given as in Table 6.1 of [35]; $Q(.)$ denotes the Gaussian function; γ is SNR of the considered system, which is given as (7) and (8) for the cases without and with cooperative communications, respectively. By changing the variable, i.e., $x=\frac{t^2}{b}$, (25) can be rewritten as

$$\mathrm{SEP}=\frac{a\sqrt{b}}{2\sqrt{2\pi}}\int_0^{\infty}\frac{F(x)}{\sqrt{x}}\exp\left(-\frac{bx}{2}\right)dx. \tag{26}$$

Based on (26), the SEPs of the considered EH-LPWA system are derived in the following Theorem 2.

Theorem 2. *The* SEP*s of the considered EH-LPWA system with energy harvesting in the cases without and with cooperative communications over Nakagami-m fading channel are, respectively, given as*

$$\begin{aligned}\mathrm{SEP}_k=&\frac{a\sqrt{b}}{2\sqrt{2\pi}}\left[\sqrt{\frac{2\pi}{b}}-\frac{\Gamma\left(m_kN+\frac{1}{2}\right)}{\Gamma(m_kN)}\left(\frac{m_k}{\Omega_k}\right)^{m_kN}\right.\\&\times\sqrt{\frac{\Omega_s\Omega_k\eta\alpha P_{\mathrm{B}}}{m_sm_kM\sigma^2(1-\alpha)d_{\mathrm{BS}}^{\beta}d_{\mathrm{SG}_k}^{\beta}}}\exp\left(\frac{m_sm_kM\sigma^2(1-\alpha)d_{\mathrm{BS}}^{\beta}d_{\mathrm{SG}_k}^{\beta}}{b\Omega_s\Omega_k\eta\alpha P_{\mathrm{B}}}\right)\\&\times\sum_{i=0}^{m_sM-1}\frac{\Gamma\left(i+\frac{1}{2}\right)}{i!}\left(\frac{b}{2}\right)^{-\frac{m_kN+i}{2}}\left(\frac{m_sM\sigma^2(1-\alpha)d_{\mathrm{BS}}^{\beta}d_{\mathrm{SG}_k}^{\beta}}{\Omega_s\eta\alpha P_{\mathrm{B}}}\right)^i\\&\times\left(\frac{m_s\Omega_kM\sigma^2(1-\alpha)d_{\mathrm{BS}}^{\beta}d_{\mathrm{SG}_k}^{\beta}}{\Omega_sm_k\eta\alpha P_{\mathrm{B}}}\right)^{\frac{m_kN-i}{2}}\\&\left.\times\mathcal{W}_{-\frac{m_kN+i}{2},\frac{m_kN-i}{2}}\left(\frac{2m_sm_kM\sigma^2(1-\alpha)d_{\mathrm{BS}}^{\beta}d_{\mathrm{SG}_k}^{\beta}}{b\Omega_s\Omega_k\eta\alpha P_{\mathrm{B}}}\right)\right],\end{aligned} \tag{27}$$

$$\begin{aligned}\mathrm{SEP}_{\mathrm{C}}=&\frac{a\sqrt{b}}{2\sqrt{2\pi}}\left[\sqrt{\frac{2\pi}{b}}-\frac{\Gamma\left(m_kKN+\frac{1}{2}\right)}{\Gamma(m_kKN)}\left(\frac{m_k}{\Omega_k}\right)^{m_kKN}\right.\\&\times\sqrt{\frac{\Omega_s\Omega_k\eta\alpha P_{\mathrm{B}}}{m_sm_kM\sigma^2(1-\alpha)d_{\mathrm{BS}}^{\beta}d_0^{\beta}}}\exp\left(\frac{m_sm_kM\sigma^2(1-\alpha)d_{\mathrm{BS}}^{\beta}d_0^{\beta}}{b\Omega_s\Omega_k\eta\alpha P_{\mathrm{B}}}\right)\\&\times\sum_{i=0}^{m_sM-1}\frac{\Gamma\left(i+\frac{1}{2}\right)}{i!}\left(\frac{b}{2}\right)^{-\frac{m_kKN+i}{2}}\left(\frac{m_sM\sigma^2(1-\alpha)d_{\mathrm{BS}}^{\beta}d_0^{\beta}}{\Omega_s\eta\alpha P_{\mathrm{B}}}\right)^i\\&\times\left(\frac{m_s\Omega_kM\sigma^2(1-\alpha)d_{\mathrm{BS}}^{\beta}d_0^{\beta}}{\Omega_sm_k\eta\alpha P_{\mathrm{B}}}\right)^{\frac{m_kKN-i}{2}}\\&\left.\times\mathcal{W}_{-\frac{m_kKN+i}{2},\frac{m_kKN-i}{2}}\left(\frac{2m_sm_kM\sigma^2(1-\alpha)d_{\mathrm{BS}}^{\beta}d_0^{\beta}}{b\Omega_s\Omega_k\eta\alpha P_{\mathrm{B}}}\right)\right],\end{aligned} \tag{28}$$

where $\mathcal{W}_{...}(.)$ *is the Whittaker functions [33].*

Proof. To obtain the SEPs of the considered EH-LPWA system, firstly, we derive the CDF, $F(x)$ in the cases of non-cooperative and cooperative communications. Based on the definition of $F(x)$, i.e.,

$$F(x)=\Pr\{\gamma<x\}, \tag{29}$$

we can easily obtain the CDFs of the considered EH-LPWA system in the cases of non-cooperative and cooperative communications by replacing γ_{th} by x in the OP expressions. Therefore, the CDFs in the cases of non-cooperative ($F_k(x)$) and cooperative ($F_{\mathrm{C}}(x)$) communications are derived as

$$\begin{aligned}F_k(x)=&1-\frac{2}{\Gamma(m_kN)}\left(\frac{m_k}{\Omega_k}\right)^{m_kN}\sum_{i=0}^{m_sM-1}\frac{1}{i!}\left(\frac{m_sM\sigma^2(1-\alpha)d_{\mathrm{BS}}^{\beta}d_{\mathrm{SG}_k}^{\beta}x}{\Omega_s\eta\alpha P_{\mathrm{B}}}\right)^i\\&\times\left(\frac{\Omega_km_sM\sigma^2(1-\alpha)d_{\mathrm{BS}}^{\beta}d_{\mathrm{SG}_k}^{\beta}x}{\Omega_sm_k\eta\alpha P_{\mathrm{B}}}\right)^{\frac{m_kN-i}{2}}\end{aligned}$$

$$\times \mathcal{K}_{m_k N-i}\left(2\sqrt{\frac{m_s m_k M\sigma^2(1-\alpha)d_{\mathrm{BS}}^{\beta}d_{\mathrm{SG}_k}^{\beta}x}{\Omega_s\Omega_k\eta\alpha P_{\mathrm{B}}}}\right), \tag{30}$$

$$F_{\mathrm{C}}(x) = 1-\frac{2}{\Gamma(m_k KN)}\left(\frac{m_k}{\Omega_k}\right)^{m_k KN}\sum_{i=0}^{m_s M-1}\frac{1}{i!}\left(\frac{m_s M\sigma^2(1-\alpha)d_{\mathrm{BS}}^{\beta}d_0^{\beta}x}{\Omega_s\eta\alpha P_{\mathrm{B}}}\right)^{i} \times\left(\frac{\Omega_k m_s M\sigma^2(1-\alpha)d_{\mathrm{BS}}^{\beta}d_0^{\beta}x}{\Omega_s m_k\eta\alpha P_{\mathrm{B}}}\right)^{\frac{m_k KN-i}{2}} \times \mathcal{K}_{m_k KN-i}\left(2\sqrt{\frac{m_s m_k M\sigma^2(1-\alpha)d_{\mathrm{BS}}^{\beta}d_0^{\beta}x}{\Omega_s\Omega_k\eta\alpha P_{\mathrm{B}}}}\right). \tag{31}$$

Replacing (30) and (31) into (26), the SEPs are now expressed as

$$\begin{aligned}\mathrm{SEP}_k =& \frac{a\sqrt{b}}{2\sqrt{2\pi}}\int_0^{\infty}\frac{\exp\left(-\frac{bx}{2}\right)}{\sqrt{x}}\left[1-\frac{2}{\Gamma(m_k N)}\left(\frac{m_k}{\Omega_k}\right)^{m_k N}\right.\\ &\times\sum_{i=0}^{m_s M-1}\frac{1}{i!}\left(\frac{m_s M\sigma^2(1-\alpha)d_{\mathrm{BS}}^{\beta}d_{\mathrm{SG}_k}^{\beta}x}{\Omega_s\eta\alpha P_{\mathrm{B}}}\right)^{i}\\ &\times\left(\frac{\Omega_k m_s M\sigma^2(1-\alpha)d_{\mathrm{BS}}^{\beta}d_{\mathrm{SG}_k}^{\beta}x}{\Omega_s m_k\eta\alpha P_{\mathrm{B}}}\right)^{\frac{m_k N-i}{2}}\\ &\left.\times\mathcal{K}_{m_k N-i}\left(2\sqrt{\frac{m_s m_k M\sigma^2(1-\alpha)d_{\mathrm{BS}}^{\beta}d_{\mathrm{SG}_k}^{\beta}x}{\Omega_s\Omega_k\eta\alpha P_{\mathrm{B}}}}\right)\right]dx\\ =&\frac{a\sqrt{b}}{2\sqrt{2\pi}}\left[\int_0^{\infty}\frac{\exp\left(-\frac{bx}{2}\right)}{\sqrt{x}}dx-\frac{2}{\Gamma(m_k N)}\left(\frac{m_k}{\Omega_k}\right)^{m_k N}\right.\\ &\times\sum_{i=0}^{m_s M-1}\frac{1}{i!}\left(\frac{m_s M\sigma^2(1-\alpha)d_{\mathrm{BS}}^{\beta}d_{\mathrm{SG}_k}^{\beta}}{\Omega_s\eta\alpha P_{\mathrm{B}}}\right)^{i}\\ &\times\left(\frac{\Omega_k m_s M\sigma^2(1-\alpha)d_{\mathrm{BS}}^{\beta}d_{\mathrm{SG}_k}^{\beta}}{\Omega_s m_k\eta\alpha P_{\mathrm{B}}}\right)^{\frac{m_k N-i}{2}}\int_0^{\infty}x^{\frac{m_k N+i-1}{2}}\exp\left(-\frac{bx}{2}\right)\\ &\left.\times\mathcal{K}_{m_k N-i}\left(2\sqrt{\frac{m_s m_k M\sigma^2(1-\alpha)d_{\mathrm{BS}}^{\beta}d_{\mathrm{SG}_k}^{\beta}x}{\Omega_s\Omega_k\eta\alpha P_{\mathrm{B}}}}\right)dx\right].\end{aligned} \tag{32}$$

$$\begin{aligned}\mathrm{SEP}_{\mathrm{C}} =& \frac{a\sqrt{b}}{2\sqrt{2\pi}}\int_0^{\infty}\frac{\exp\left(-\frac{bx}{2}\right)}{\sqrt{x}}\left[1-\frac{2}{\Gamma(m_k KN)}\left(\frac{m_k}{\Omega_k}\right)^{m_k KN}\right.\\ &\times\sum_{i=0}^{m_s M-1}\frac{1}{i!}\left(\frac{m_s M\sigma^2(1-\alpha)d_{\mathrm{BS}}^{\beta}d_0^{\beta}x}{\Omega_s\eta\alpha P_{\mathrm{B}}}\right)^{i}\\ &\times\left(\frac{\Omega_k m_s M\sigma^2(1-\alpha)d_{\mathrm{BS}}^{\beta}d_0^{\beta}x}{\Omega_s m_k\eta\alpha P_{\mathrm{B}}}\right)^{\frac{m_k KN-i}{2}}\\ &\left.\times\mathcal{K}_{m_k KN-i}\left(2\sqrt{\frac{m_s m_k M\sigma^2(1-\alpha)d_{\mathrm{BS}}^{\beta}d_0^{\beta}x}{\Omega_s\Omega_k\eta\alpha P_{\mathrm{B}}}}\right)\right]dx\\ =&\frac{a\sqrt{b}}{2\sqrt{2\pi}}\left[\int_0^{\infty}\frac{\exp\left(-\frac{bx}{2}\right)}{\sqrt{x}}dx-\frac{2}{\Gamma(m_k KN)}\left(\frac{m_k}{\Omega_k}\right)^{m_k KN}\right.\\ &\times\sum_{i=0}^{m_s M-1}\frac{1}{i!}\left(\frac{m_s M\sigma^2(1-\alpha)d_{\mathrm{BS}}^{\beta}d_0^{\beta}}{\Omega_s\eta\alpha P_{\mathrm{B}}}\right)^{i}\\ &\times\left(\frac{\Omega_k m_s M\sigma^2(1-\alpha)d_{\mathrm{BS}}^{\beta}d_0^{\beta}}{\Omega_s m_k\eta\alpha P_{\mathrm{B}}}\right)^{\frac{m_k KN-i}{2}}\int_0^{\infty}x^{\frac{m_k KN+i-1}{2}}\exp\left(-\frac{bx}{2}\right)\\ &\left.\times\mathcal{K}_{m_k KN-i}\left(2\sqrt{\frac{m_s m_k M\sigma^2(1-\alpha)d_{\mathrm{BS}}^{\beta}d_0^{\beta}x}{\Omega_s\Omega_k\eta\alpha P_{\mathrm{B}}}}\right)dx\right].\end{aligned} \tag{33}$$

Now, applying [33, Eq. (3.361.2)], the first integral in (32) and (33) can be found as

$$\int_0^{\infty}\frac{\exp\left(-\frac{bx}{2}\right)}{\sqrt{x}}dx=\sqrt{\frac{2\pi}{b}}. \tag{34}$$

Then, applying [33, Eq. (6.643.3)], two second integrals in (32) and (33) are now calculated as

$$\begin{aligned}&\int_0^{\infty}x^{\frac{m_k N+i-1}{2}}\exp\left(-\frac{bx}{2}\right)\mathcal{K}_{m_k N-i}\left(2\sqrt{\frac{m_s m_k M\sigma^2(1-\alpha)d_{\mathrm{BS}}^{\beta}d_{\mathrm{SG}_k}^{\beta}x}{\Omega_s\Omega_k\eta\alpha P_{\mathrm{B}}}}\right)dx\\ &=\Gamma\left(m_k N+\frac{1}{2}\right)\Gamma\left(i+\frac{1}{2}\right)\exp\left(\frac{m_s m_k M\sigma^2(1-\alpha)d_{\mathrm{BS}}^{\beta}d_{\mathrm{SG}_k}^{\beta}}{b\Omega_s\Omega_k\eta\alpha P_{\mathrm{B}}}\right)\left(\frac{b}{2}\right)^{-\frac{m_k N+i}{2}}\\ &\times\frac{1}{2\sqrt{\frac{m_s m_k M\sigma^2(1-\alpha)d_{\mathrm{BS}}^{\beta}d_{\mathrm{SG}_k}^{\beta}}{\Omega_s\Omega_k\eta\alpha P_{\mathrm{B}}}}}\mathcal{W}_{-\frac{m_k N+i}{2},\frac{m_k N-i}{2}}\left(\frac{2m_s m_k M\sigma^2(1-\alpha)d_{\mathrm{BS}}^{\beta}d_{\mathrm{SG}_k}^{\beta}}{b\Omega_s\Omega_k\eta\alpha P_{\mathrm{B}}}\right),\end{aligned} \tag{35}$$

$$\begin{aligned}&\int_0^{\infty}x^{\frac{m_k KN+i-1}{2}}\exp\left(-\frac{bx}{2}\right)\mathcal{K}_{m_k KN-i}\left(2\sqrt{\frac{m_s m_k M\sigma^2(1-\alpha)d_{\mathrm{BS}}^{\beta}d_0^{\beta}x}{\Omega_s\Omega_k\eta\alpha P_{\mathrm{B}}}}\right)dx\\ &=\Gamma\left(m_k KN+\frac{1}{2}\right)\Gamma\left(i+\frac{1}{2}\right)\exp\left(\frac{m_s m_k M\sigma^2(1-\alpha)d_{\mathrm{BS}}^{\beta}d_0^{\beta}}{b\Omega_s\Omega_k\eta\alpha P_{\mathrm{B}}}\right)\left(\frac{b}{2}\right)^{-\frac{m_k KN+i}{2}}\\ &\times\frac{1}{2\sqrt{\frac{m_s m_k M\sigma^2(1-\alpha)d_{\mathrm{BS}}^{\beta}d_0^{\beta}}{\Omega_s\Omega_k\eta\alpha P_{\mathrm{B}}}}}\mathcal{W}_{-\frac{m_k KN+i}{2},\frac{m_k KN-i}{2}}\left(\frac{2m_s m_k M\sigma^2(1-\alpha)d_{\mathrm{BS}}^{\beta}d_0^{\beta}}{b\Omega_s\Omega_k\eta\alpha P_{\mathrm{B}}}\right).\end{aligned} \tag{36}$$

Replacing (34), (35) and (36) into (32) and (33), we obtain the SEPs of the considered system as in Theorem 2. The proof is thus completed.

4. Optimizing the time-switching ratio

Since the performance of the considered EH-LPWA system depends on the time switching ratio α, in this section, we derive the optimal value of α that minimizes the OPs. In particular, we will find an optimal value of α (denoted by α^*) to achieve lowest OPs. Consequently, the SEPs will be minimum and the throughputs will be maximum with α^*.

The optimization problem for improving the performance of the considered EH-LPWA system can be expressed as

$$\begin{aligned}&\min\ \mathcal{P}_k, \mathcal{P}_{\mathrm{C}}.\\ &s.t.\ 0<\alpha<1\end{aligned} \tag{37}$$

To solve this optimization problem, the linear programming method is applied to derive α^*, i.e.,

$$\alpha_k^* = \arg\ \min_{\alpha}\mathcal{P}_k, \tag{38}$$

$$\alpha_{\mathrm{C}}^* = \arg\ \min_{\alpha}\mathcal{P}_{\mathrm{C}}, \tag{39}$$

where α_k^* and α_{C}^* are, respectively, the optimal values of α for the considered EH-LPWA system without and with cooperative communications. The calculation method to obtain α^* for both the cases without and with cooperative communications is summarized in Algorithm 1 as follows.

Algorithm 1 Optimal Time Switching Ratio Calculation Algorithm

1: Solve $\frac{\partial \mathcal{P}}{\partial \alpha} = 0$ for $\alpha = \alpha_0$;
2: **if** $\begin{cases} 0 < \alpha_0 < 1 \\ \frac{\partial \mathcal{P}}{\partial \alpha} < 0 \text{ for } \alpha < \alpha_0 \\ \frac{\partial \mathcal{P}}{\partial \alpha} < 0 \text{ for } \alpha > \alpha_0 \end{cases}$
3: **then**
4: Output optimal value $\alpha^* = \alpha_0$;
5: **else**
6: Output optimal value $\alpha^* = \emptyset$;
7: **end**

It is worth noticing that in the case of $\alpha^* = \emptyset$ (where $\emptyset$ is the empty set), there is not any value of α^* for the considered EH-LPWA system. Thus, based on the certain feature of the expression $\frac{\partial \mathcal{P}}{\partial \alpha}$, we can choose a suitable value of α to improve the performance of the considered EH-LPWA system.

On the other hand, since the OP expressions given in (13) and (14) are very complex, it is too difficult to take the derivative from these expressions. Therefore, before taking the derivative of OP expressions with respect to α, we use approximate functions to reduce the complexity of the OP expressions. In particular, the Bessel function can be approximated as [36]

$$\mathcal{K}_n(x) \approx \frac{(n-1)!}{2}\left(\frac{x}{2}\right)^{-n}. \tag{40}$$

Then, the OP expressions given in (13) and (14) are, respectively, approximated as

$$\begin{aligned}\mathcal{P}_k^{\text{ap}} \approx & 1 - \frac{2}{\Gamma(m_k N)}\left(\frac{m_k}{\Omega_k}\right)^{m_k N}\sum_{i=0}^{m_s M-1}\frac{1}{i!}\left(\frac{m_s M\sigma^2(1-\alpha)d_{\text{BS}}^{\beta}d_{\text{SG}_k}^{\beta}\gamma_{\text{th}}}{\Omega_s\eta\alpha P_{\text{B}}}\right)^{i} \\ & \times\left(\frac{\Omega_k m_s M\sigma^2(1-\alpha)d_{\text{BS}}^{\beta}d_{\text{SG}_k}^{\beta}\gamma_{\text{th}}}{\Omega_s m_k\eta\alpha P_{\text{B}}}\right)^{\frac{m_k N-i}{2}} \\ & \times\frac{(m_k N-i-1)!}{2}\left(\sqrt{\frac{m_s m_k M\sigma^2(1-\alpha)d_{\text{BS}}^{\beta}d_{\text{SG}_k}^{\beta}\gamma_{\text{th}}}{\Omega_s\Omega_k\eta\alpha P_{\text{B}}}}\right)^{-m_k N+i} \\ = & 1 - \frac{1}{\Gamma(m_k N)}\left(\frac{m_k}{\Omega_k}\right)^{m_k N}\sum_{i=0}^{m_s M-1}\frac{(m_k N-i-1)!}{i!} \\ & \times\left(\frac{m_s M\sigma^2(1-\alpha)d_{\text{BS}}^{\beta}d_{\text{SG}_k}^{\beta}\gamma_{\text{th}}}{\Omega_s\eta\alpha P_{\text{B}}}\right)^{i}\left(\frac{\Omega_k}{m_k}\right)^{m_k N-i}.\end{aligned} \tag{41}$$

$$\begin{aligned}\mathcal{P}_{\text{C}}^{\text{ap}} \approx & 1 - \frac{2}{\Gamma(m_k KN)}\left(\frac{m_k}{\Omega_k}\right)^{m_k KN}\sum_{i=0}^{m_s M-1}\frac{1}{i!}\left(\frac{m_s M\sigma^2(1-\alpha)d_{\text{BS}}^{\beta}d_0^{\beta}\gamma_{\text{th}}}{\Omega_s\eta\alpha P_{\text{B}}}\right)^{i} \\ & \times\left(\frac{\Omega_k m_s M\sigma^2(1-\alpha)d_{\text{BS}}^{\beta}d_0^{\beta}\gamma_{\text{th}}}{\Omega_s m_k\eta\alpha P_{\text{B}}}\right)^{\frac{m_k KN-i}{2}} \\ & \times\frac{(m_k KN-i-1)!}{2}\left(\sqrt{\frac{m_s m_k M\sigma^2(1-\alpha)d_{\text{BS}}^{\beta}d_0^{\beta}\gamma_{\text{th}}}{\Omega_s\Omega_k\eta\alpha P_{\text{B}}}}\right)^{-m_k KN+i} \\ = & 1 - \frac{1}{\Gamma(m_k KN)}\left(\frac{m_k}{\Omega_k}\right)^{m_k KN}\sum_{i=0}^{m_s M-1}\frac{(m_k KN-i-1)!}{i!} \\ & \times\left(\frac{m_s M\sigma^2(1-\alpha)d_{\text{BS}}^{\beta}d_0^{\beta}\gamma_{\text{th}}}{\Omega_s\eta\alpha P_{\text{B}}}\right)^{i}\left(\frac{\Omega_k}{m_k}\right)^{m_k KN-i}.\end{aligned} \tag{42}$$

Then, taking the derivative of $\frac{\partial \mathcal{P}_k^{\text{ap}}}{\partial \alpha}$ and $\frac{\partial \mathcal{P}_{\text{C}}^{\text{ap}}}{\partial \alpha}$ with $\gamma_{\text{th}} = 2^{\frac{\mathcal{R}}{1-\alpha}} - 1$, we have

$$\begin{aligned}\frac{\partial \mathcal{P}_k^{\text{ap}}}{\partial \alpha} = & -\frac{1}{\Gamma(m_k N)}\left(\frac{m_k}{\Omega_k}\right)^{m_k N}\sum_{i=0}^{m_s M-1}\frac{i(m_k N-i-1)!}{i!}\left(\frac{\Omega_k}{m_k}\right)^{m_k N-i} \\ & \times\left(\frac{m_s M\sigma^2(1-\alpha)d_{\text{BS}}^{\beta}d_{\text{SG}_k}^{\beta}\gamma_{\text{th}}}{\Omega_s\eta\alpha P_{\text{B}}}\right)^{i-1} \\ & \times\frac{m_s M\sigma^2 d_{\text{BS}}^{\beta}d_{\text{SG}_k}^{\beta}}{\Omega_s\eta P_{\text{B}}} \\ & \times\left[-\frac{1}{\alpha^2}\left(2^{\frac{\mathcal{R}}{1-\alpha}}-1\right)+\frac{1-\alpha}{\alpha}\left(2^{\frac{\mathcal{R}}{1-\alpha}}-1\right)\frac{\mathcal{R}}{(1-\alpha)^2}\ln 2\right].\end{aligned} \tag{43}$$

$$\begin{aligned}\frac{\partial \mathcal{P}_{\text{C}}^{\text{ap}}}{\partial \alpha} = & -\frac{1}{\Gamma(m_k KN)}\left(\frac{m_k}{\Omega_k}\right)^{m_k KN}\sum_{i=0}^{m_s M-1}\frac{i(m_k KN-i-1)!}{i!}\left(\frac{\Omega_k}{m_k}\right)^{m_k KN-i} \\ & \times\left(\frac{m_s M\sigma^2(1-\alpha)d_{\text{BS}}^{\beta}d_0^{\beta}\gamma_{\text{th}}}{\Omega_s\eta\alpha P_{\text{B}}}\right)^{i-1} \\ & \times\frac{m_s M\sigma^2 d_{\text{BS}}^{\beta}d_0^{\beta}}{\Omega_s\eta P_{\text{B}}} \\ & \times\left[-\frac{1}{\alpha^2}\left(2^{\frac{\mathcal{R}}{1-\alpha}}-1\right)+\frac{1-\alpha}{\alpha}\left(2^{\frac{\mathcal{R}}{1-\alpha}}-1\right)\frac{\mathcal{R}}{(1-\alpha)^2}\ln 2\right].\end{aligned} \tag{44}$$

From (43) and (44), it can be easily shown that $\frac{\partial \mathcal{P}_k^{\text{ap}}}{\partial \alpha} = 0$ and $\frac{\partial \mathcal{P}_{\text{C}}^{\text{ap}}}{\partial \alpha} = 0$ when

$$-\frac{1}{\alpha^2}\left(2^{\frac{\mathcal{R}}{1-\alpha}}-1\right)+\frac{1-\alpha}{\alpha}\left(2^{\frac{\mathcal{R}}{1-\alpha}}-1\right)\frac{\mathcal{R}}{(1-\alpha)^2}\ln 2 = 0. \tag{45}$$

Now, we rewrite (45) as

$$\frac{1}{\alpha} = \frac{\mathcal{R}\ln 2}{1-\alpha}. \tag{46}$$

Then, we can easily obtain α_0 from (46) as

$$\alpha_0 = \frac{1}{1+\mathcal{R}\ln 2}. \tag{47}$$

Since α_0 satisfies the second condition in Algorithm 1, this is the optimal value of the time switching ratio of the considered EH-LPWA system. In other words, we have

$$\alpha_k^* = \alpha_{\text{C}}^* = \alpha^* = \alpha_0 = \frac{1}{1+\mathcal{R}\ln 2}. \tag{48}$$

5. Numerical results and discussions

In this section, the performance of the considered EH-LPWA system is evaluated via mathematical expressions in the previous section. To demonstrate the correctness of our derived expressions, the Monte-Carlo simulations are also provided in all investigated scenarios using 10^7 channel realizations. In all scenarios, the average SNR is calculated as the ratio between the average transmit power of the power beacon and the noise power, i.e., SNR $= P_{\text{B}}/\sigma^2$. Since the power beacon is a power transmit station, the transmit power of the power beacon can be high. Thus, the SNR range is set from 0 to 40 dB. Meanwhile, the transmit power of LoRa transmitters is often lower than 10 dBm in practical scenarios. Additionally, the energy harvesting efficiency is chosen as $\eta = 0.85$.[3] Other parameters are varied to investigate their impacts on the OPs and SEPs of the considered EH-LPWA system. To clarify, the simulation parameters are listed in Table 1.

Fig. 3 illustrates the OPs of the considered EH-LPWA system versus the average SNR with four gateways ($K = 4$). The transmit and receive antennas at B and G are chosen as $M = N = 3$. The distances are

[3] In practice, the energy harvesting efficiency η depends on the rectification process and the energy harvesting circuitry. The measurements and experiments demonstrated that, it ranges from 0.13 to 0.95 [37]. Therefore, it is often selected as 0.5 [6,38], 0.8 [10], or 1 [7]. Thus, the assumption $\eta = 0.85$ in this paper is still valid for consideration. However, it may be lower than 0.85 in practical scenarios.

Table 1
Simulation parameters for evaluating the system performance.

Notation	Description	Fixed value	Varying range
SNR	Signal-to-noise ratio	30 dB	20, 25 dB; 0 ~ 40 dB
σ^2	Variance of Gaussian noise	1	None
η	Energy harvesting efficiency	0.85	None
α	Time switching ratio	0.5	0.1 ~ 0.9
d_{BS}	Distance between B and S	1	None
d_{SG_k}	Distance from S to the kth gateway	2	3, 4, 5
β	Path-loss exponent	3	2
K	Number of gateways	4	2
M	Number of transmit antennas at B	3	2, 4
N	Number of receive antennas at kth gateway	3	2, 4
$\mathcal{R}$	Pre-defined data transmission rate	1.5 bit/s/Hz	1, 2, 3 bit/s/Hz
(a, b)	A couple of the modulation types	(2, 1)	(3, 1/5)
m_s, m_k	Nakagami parameters	2	1
Ω_s, Ω_k	Average channel gains	2	1

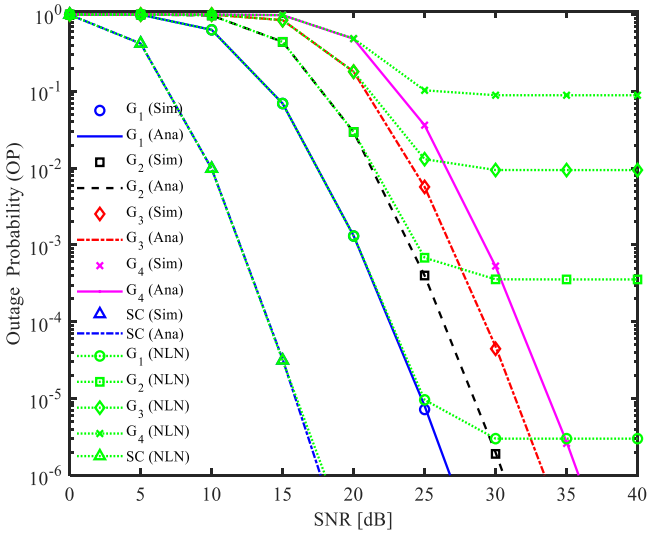

Fig. 3. The OPs of the considered EH-LPWA system versus the average SNR for $K = 4$, $M = N = 3$, $d_{\mathrm{BS}} = 1$, $d_{\mathrm{SG}_1} = 3$, $d_{\mathrm{SG}_2} = 4$, $d_{\mathrm{SG}_3} = 5$, $d_{\mathrm{SG}_4} = 6$, $\beta = 3$, $\alpha = 0.5$, $\Omega_s = \Omega_k = 2$, $m_s = m_k = 2$, $P_{\mathrm{th}} = 30$ dBm, $\mathcal{R} = 1.5$ bit/s/Hz.

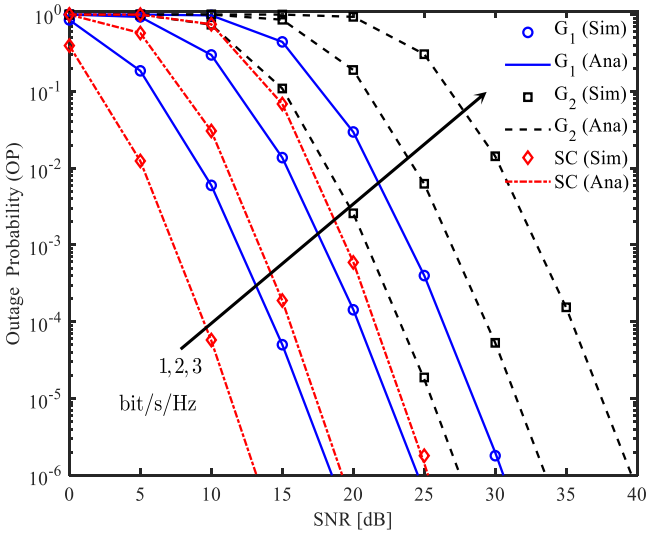

Fig. 4. The impact of data transmission rates on the OPs of the considered EH-LPWA system, for $K = 2$, $M = N = 3$, $d_{\mathrm{BS}} = 1$, $d_{\mathrm{SG}_1} = 2$, $d_{\mathrm{SG}_2} = 4$, $\beta = 3$, $\alpha = 0.5$, $\Omega_s = \Omega_k = 2$, $m_s = m_k = 2$, $\mathcal{R} = 1, 2, 3$ bit/s/Hz.

$d_{\mathrm{BS}} = 1$, $d_{\mathrm{SG}_1} = 2$, $d_{\mathrm{SG}_2} = 3$, $d_{\mathrm{SG}_3} = 4$, $d_{\mathrm{SG}_4} = 5$,[4] and the path loss exponent is $\beta = 3$. The time switching ratio is $\alpha = 0.5$.[5] The predefined data transmission rate is $\mathcal{R} = 1.5$ bit/s/Hz.[6] The analysis curves in Fig. 3 are plotted by using (13) and (14) corresponding to the OPs at gateways (denoted by G_1, G_2, G_3, and G_4) and the server center (denoted by SC), respectively. Meanwhile, the markers denote the simulation results. Additionally, the OPs of the considered EH-LPWA system with nonlinear energy harvester are also provided with the saturation power threshold $P_{\mathrm{th}} = 30$ dBm for convenience in the comparison with those when using linear energy harvesters. It is obvious from Fig. 3, the distances have a great impact on the OPs of the considered EH-LPWA system because the OP of G_1 significantly lower than that of G_4. Also, the cooperative communications can remarkably improve the performance of the considered EH-LPWA system. Specifically, when the OP requirement is 10^{-3}, the case of cooperative communications only needs SNR = 17 dB, meanwhile, G_1, G_2, G_3, and G_4 need 27, 32, 35, and 38 dB, respectively, to satisfy this requirement. Since the received signal power at the server center is significantly enhanced with cooperative communications, the performance in the case with cooperative communications is much better than that in the case without cooperative communications. In other words, γ_{C} given in (8) is greatly higher than γ_{G_k} given in (7), the OP with cooperative communications is significantly lower than that without cooperative communications. An important observation from Fig. 3 is that, under the impact of saturation power threshold, the OPs with nonlinear energy harvester reach the error floors in the high SNR regime, especially in the cases without cooperative communications.

Fig. 4 presents the impact of data transmission rates on the OPs of the EH-LPWA system for $\mathcal{R} = 1, 2, 3$ bit/s/Hz. For easy observation, we choose $K = 2$ gateways. It can be seen that the high OPs can be achieved with high data transmission rates. In other words, the usage

[4] As presented in [35, Eq. (2.29)], the unit of the distance depends on a certain reference distance. Thus, most of works such as [25,39] neglected the unit of the distance.

[5] It is noteworthy that the system parameters are chosen by measurements and experiments in practice. Specifically, the distances are often nominalized [39] or selected from 1 to 3 [12]. The path loss exponent ranges from 2 to 6, thus, many works chose it as $\beta = 2.5$ [10], $\beta = 2.7$ [12,39], and $\beta = 3$ [25]. For half-duplex transmission, the time switching ratio α is often chosen from 0.3 to 0.5 because this range can minimize the OP (or SEP) and maximize the throughput of the half-duplex wireless systems [39,40]. Similar to the measurements and experiments reported in previous works [6,7,12,25,38,39], in this paper, we use $\beta = 2$ or 3, $\alpha = 0.5$ and $\eta = 0.85$ for the system evaluations. On the other hand, we also change the value of α from 0.1 to 0.9 to determine its impact on the OP of the considered EH-LPWA system.

[6] Note that the predefined data transmission rates are corresponding to the modulation types and the bandwidth. For example, $\mathcal{R} = 1.5$ bit/s/Hz is equivalent to transmit 3 bits (8-QAM) per second via a bandwidth of 2 Hz. Similarly, $\mathcal{R} = 1, 2$, and 3 bit/s/Hz are equivalent to transmit 1, 2, and 3 bits (corresponding to BPSK, 4-QAM, and 8-QAM) per second via a bandwidth of 1 Hz.

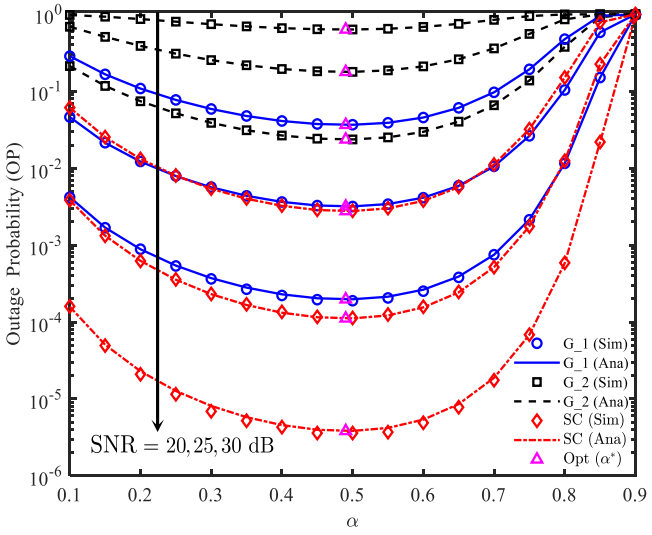

Fig. 5. The OPs of the considered EH-LPWA system versus the time switching ratio α for different SNRs, $K = 2$, $M = N = 3$, $d_{\text{BS}} = 1$, $d_{\text{SG}_1} = 2$, $d_{\text{SG}_2} = 4$, $\beta = 3$, $\Omega_s = \Omega_k = 1$, $m_s = m_k = 1$, $\mathcal{R} = 1.5$ bit/s/Hz.

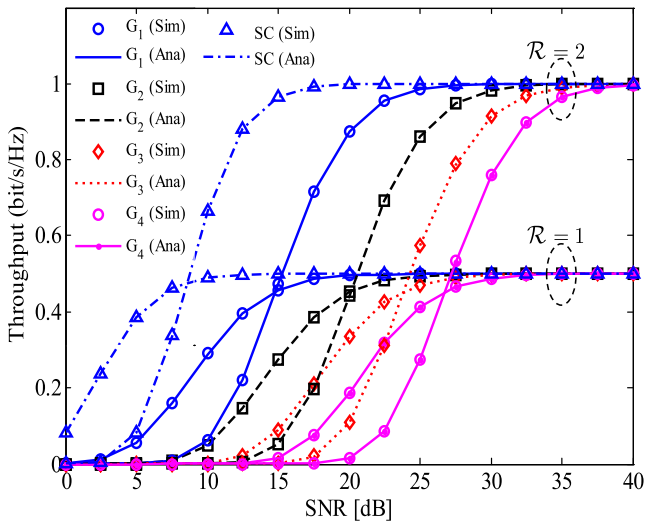

Fig. 6. The throughput of the considered EH-LPWA system versus the average SNR for two data transmission rates, $K = 4$, $M = N = 3$, $d_{\text{BS}} = 1$, $d_{\text{SG}_1} = 2$, $d_{\text{SG}_2} = 3$, $d_{\text{SG}_3} = 4$, $d_{\text{SG}_4} = 5$, $\beta = 3$, $\alpha = 0.5$, $\Omega_s = \Omega_k = 1$, $m_s = m_k = 1$, $\mathcal{R} = 1, 2$ bit/s/Hz.

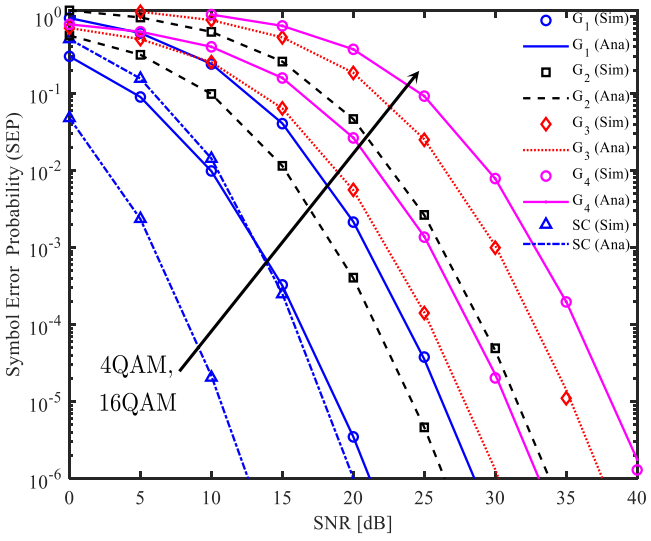

Fig. 7. The SEPs of the considered EH-LPWA system versus the average SNR for two modulation schemes, $K = 4$, $M = N = 3$, $d_{\text{BS}} = 1$, $d_{\text{SG}_1} = 2$, $d_{\text{SG}_2} = 3$, $d_{\text{SG}_3} = 4$, $d_{\text{SG}_4} = 5$, $\beta = 3$, $\alpha = 0.5$, $\Omega_s = \Omega_k = 2$, $m_s = m_k = 2$.

of high data transmission rates greatly reduces the performance of the considered EH-LPWA system. Particularly, at SNR = 40 dB, the OP at G_2 is only 10^{-2} for $\mathcal{R} = 3$ bit/s/Hz while it is nearly 10^{-5} for $\mathcal{R} = 1$ bit/s/Hz. On the other hand, the OPs at G_1 in the cases of $\mathcal{R} = 1$ bit/s/Hz and $\mathcal{R} = 2$ bit/s/Hz are similar with the OPs at server center in the cases of $\mathcal{R} = 2$ bit/s/Hz and $\mathcal{R} = 3$ bit/s/Hz, respectively. Therefore, depending on the requirements of the considered EH-LPWA system in practice, we can choose the cases with or without cooperative communications corresponding to the suitable data transmission rate to reduce the signal processing complexity. For example, when SNR is fixed at SNR = 25 dB and the OP is required as 10^{-3}, we can either use one gateway (G_1) and choose $\mathcal{R} = 1$ bit/s/Hz to avoid the signal processing complexity at the server center or use the cooperative communications with two gateways and the higher data transmission rate ($\mathcal{R} = 2$ bit/s/Hz).

Fig. 5 determines the impact of the time switching ratio α on the OPs of the considered EH-LPWA system for different SNRs, i.e., SNR = 20, 25, 30 dB. Herein, we use (48) to derive the OP curves with the optimal value of α. Be noted that in the case of $\Omega_s = \Omega_k = 1$ and $m_s = m_k = 1$, the Nakagami-m fading channels become the Rayleigh fading channels. As observed from Fig. 5, the OPs are minimum when $\alpha = \alpha^* = 0.49 \approx 0.5$ for the investigated parameters (calculated from (48)). In other words, the usage a half of one transmission block for EH is optimal for the considered EH-LPWA system. It is reasonable because the performance of the system depends on both α and the transmit power of the sensor. When α is low, the time duration for EH is low and the time duration for signal transmission is high, leading to the low transmit power of the sensor. Thus, the OP performance is also low. When α is higher, the time duration is higher for EH, but it is lower for signal transmission. Consequently, the transmit power of the sensor is higher but it is difficult to detect successfully the received signals at the gateways because of the lower time duration for signal transmission. On the other hand, in the case that we cannot use the optimal value of α ($\alpha = 0.5$), we can use $\alpha < 0.5$ to achieve better performance of the considered EH-LPWA system. It is because the OPs with $\alpha = 0.2, 0.4$ are lower than those with $\alpha = 0.8, 0.6$, respectively.

In Fig. 6, we evaluate the throughput of the considered EH-LPWA system, where the throughput is computed as $\mathcal{T} = \mathcal{R}(1-\alpha)(1-\mathcal{P})$, herein, $\mathcal{P}$ is given as (13) and (14) for the cases without and with cooperative communications, respectively. Since $\alpha = 0.5$, there is only a half of transmission block for transmitting signals, thus, the throughput is reduced by a half in comparison with the case without energy harvesting. It can be seen from this figure that in the case of low data transmission rate, i.e., $\mathcal{R} = 1$ bit/s/Hz, all gateways and server center can get a half of the target throughput at SNR > 30 dB. However, with the higher data transmission rate, i.e., $\mathcal{R} = 2$ bit/s/Hz, it needs SNR = 38 dB to achieve a half of the target throughput for all gateways and the server center. On the other hand, the differences between the throughput of all gateways are significant in the low SNR regime, especially for $\mathcal{R} = 2$ bit/s/Hz. Another observation from Figs. 3–6 is that the higher data transmission rates can be chosen, i.e., $\mathcal{R} = 4, 5, \ldots$ bit/s/Hz. Although higher $\mathcal{R}$ will reduce the OP and throughput performance of the considered EH-LPWA system, the features of the OP and throughput curves are still similar to those in the case of $\mathcal{R} = 1, 2$, and 3 bit/s/Hz. Thus, we often use $\mathcal{R} = 1, 2$, and 3 bit/s/Hz in most figures for the easy observation.

The SEPs of the considered EH-LPWA system versus the average SNR for two modulation schemes, i.e., 4-QAM ($a = 2, b = 1$) and 16-QAM ($a = 3, b = 1/5$), are illustrated in Fig. 7. We use (27) and

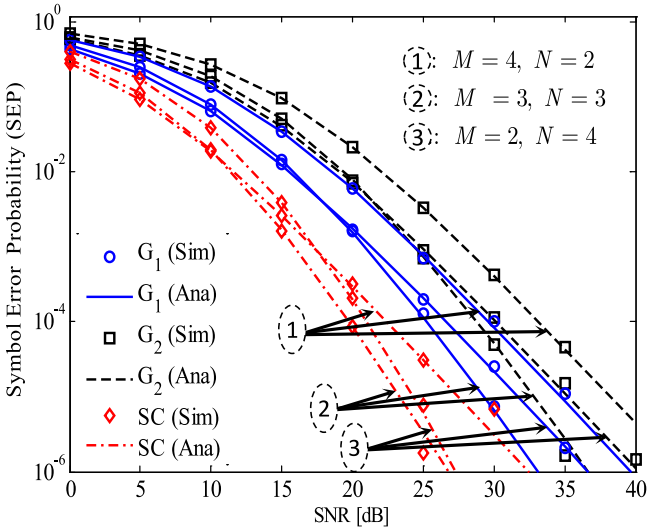

Fig. 8. The impacts of number of transmit antennas at power beacon and number of received antennas at gateways on the SEPs of the considered EH-LPWA system, $K = 2$, $d_{\mathrm{BS}} = 1$, $d_{\mathrm{SG}_1} = 2$, $d_{\mathrm{SG}_2} = 3$, $\beta = 2$, $\alpha = 0.5$, $\Omega_s = \Omega_k = 1$, $m_s = m_k = 1$.

(28) to plot the analysis curves of SEPs in the cases without and with the cooperative communications, respectively. Similar to the OPs, with the higher order modulation scheme, the higher SEPs can be achieved. In particular, the diversity order of the G_1, G_2, and the cooperative communication system is three, which is equal to the number of receive antennas at G_1 and G_2. Meanwhile, the diversity order of the G_3 and G_4 is two, it is less than the number of receive antennas at G_3 and G_4. These results are reasonable, because the distances from sensor to G_1 and G_2 are less than these from sensor to G_3 and G_4 ($d_{\mathrm{SG}_1} = 2$, $d_{\mathrm{SG}_2} = 3$, $d_{\mathrm{SG}_3} = 4$, $d_{\mathrm{SG}_4} = 5$).

Fig. 8 investigates the impacts of the number of transmit antennas at power beacon and the number of receive antennas at gateways on the SEPs of the considered EH-LPWA system with $M + N = 6$, using 4-QAM. As shown from Fig. 8, the case of $M = N = 3$ (circle two in this figure) is the best case and the case of $M = 4, N = 2$ (circle one in this figure) is the worst case among three considered cases. These results are reasonable for the considered EH-LPWA system. It is because the performance of the considered system is improved when the SNRs at the kth gateway and the server center increase. Meanwhile, these SNR values depend on the transmit power of IoT sensor (P_{S}) and SG_k channel gains ($\|\mathbf{h}_{\mathrm{SG}_k}\|^2$). When M increases, the harvested energy at S will increase leading to P_{S} increases. Similarly, when N increases, the received signal power at the gateways will be increased because $\|\mathbf{h}_{\mathrm{SG}_k}\|^2$ increases. As the results, when $M + N$ is a constant, we need to find the certain values of M and N to achieve the best performance of the considered system. In that context, the case of $M = N = 3$ is the best case in among three investigated cases because this the case can balance both P_{S} and $\|\mathbf{h}_{\mathrm{SG}_k}\|^2$. In other words, in the case of $M = 4, N = 2$, P_{S} increases but $\|\mathbf{h}_{\mathrm{SG}_k}\|^2$ significantly decreases in comparison with the case of $M = N = 3$, thus, the performance in the case of $M = 4, N = 2$ is lower than that of $M = N = 3$. Similarly, in the case of $M = 2, N = 4$, although $\|\mathbf{h}_{\mathrm{SG}_k}\|^2$ increases but P_{S} greatly reduces in comparison with the case of $M = N = 3$, thus, the performance in the case of $M = 2, N = 4$ is also lower than that of $M = N = 3$. From this observation, we can use the number of transmit antennas at power beacon equal to the number of receive antennas at gateways to achieve the best performance of the considered EH-LPWA system.

6. Conclusion

Applying energy harvesting for sensor in IoT systems is inevitable for future wireless networks, especially for low-power wide-are systems. Therefore, in this paper, we exploit EH for LPWA system and mathematically analyze the performance of the EH-LPWA system by deriving the exact closed-form expressions of outage probability, throughput, and symbol error probability to clearly show the system behaviors for both cases without and with cooperative communications. Notably, we obtained the optimal time switching ratio to minimize the OPs, SEPs and maximizes the throughputs of the considered EH-LPWA system. Numerical results have confirmed that the distances and the data transmission rates have great impacts on the OPs, throughputs, and SEPs of the considered EH-LPWA system. Specifically, the usage of a half of time duration of transmission block for energy harvesting can achieve the best performance for the EH-LPWA system. Also, due to the time duration for energy harvesting, the considered EH-LPWA system throughput cannot reach the target throughput. In addition, the diversity order of the considered EH-LPWA system in the case without cooperative communications can be equal to the number of receive antennas at the gateways for certain distances. Furthermore, the usage of cooperative communications significantly improve the performance of the considered system. We also pointed out that, by using a number of transmit antennas at the power beacon equal to the number of receive antennas at gateways, the best performance of the considered EH-LPWA system can be achieved.

Declaration of competing interest

The authors declare that they have no known competing financial interests or personal relationships that could have appeared to influence the work reported in this paper.

Data availability

The data used to support the findings of this study are available from the corresponding author upon request.

Acknowledgments

This publication is the output of the ASEAN IVO (http://www.nict.go.jp/en/asean_ivo/index.html) project, “An energy efficient, self-sustainable, and long range IoT system for drought monitoring and early warning”, and financially supported by NICT, Viet Nam (http://www.nict.go.jp/en/index.html)

References

[1] Clerckx B, Zhang R, Schober R, Ng DWK, Kim DI, Poor HV. Fundamentals of wireless information and power transfer: From RF energy harvester models to signal and system designs. IEEE J Sel Areas Commun 2018;37(1):4–33.
[2] Pham Q-V, Fang F, Ha VN, Piran MJ, Le M, Le LB, Hwang W-J, Ding Z. A survey of multi-access edge computing in 5G and beyond: Fundamentals, technology integration, and state-of-the-art. IEEE Access 2020;8:116974–7017.
[3] Ishibashi K, Manyvone D, Itoh M, Dao V-L, Hoang V-P. Beat sensors for smart environment monitoring systems. In: 2019 3rd international conference on recent advances in signal processing, telecommunications computing (SigTelCom). 2019, p. 77–9.
[4] Lu X, Wang P, Niyato D, Kim DI, Han Z. Wireless networks with RF energy harvesting: A contemporary survey. IEEE Commun Surv Tutor 2014;17(2):757–89.
[5] Nguyen V-D, Duong TQ, Tuan HD, Shin O-S, Poor HV. Spectral and energy efficiencies in full-duplex wireless information and power transfer. IEEE Trans Commun 2017;65(5):2220–33.
[6] Ni Z, Motani M. Performance of energy harvesting receivers with power optimization. IEEE Trans Commun 2018;66(3):1309–21.
[7] Ko H, Pack S. A software-defined surveillance system with energy harvesting: Design and performance optimization. IEEE Internet Things J 2018;5(3):1361–9.
[8] Nguyen BC, Tran XN, et al. On the performance of roadside unit-assisted energy harvesting full-duplex amplify-and-forward vehicle-to-vehicle relay systems. AEU-Int J Electron Commun 2020;153289.
[9] Alsaba Y, Leow CY, Rahim SKA. Full-duplex cooperative non-orthogonal multiple access with beamforming and energy harvesting. IEEE Access 2018;6:19726–38.
[10] Dong Y, Hossain MJ, Cheng J. Performance of wireless powered amplify and forward relaying over Nakagami-m fading channels with nonlinear energy harvester. IEEE Commun Lett 2016;20(4):672–5.

[11] Nguyen BC, Hoang TM, Tran PT, Nguyen TN. Outage probability of NOMA system with wireless power transfer at source and full-duplex relay. AEU - Int J Electron Commun 2020;116:152957.
[12] Babaei M, Aygölü U, Başaran M, Durak-Ata L. BER performance of full-duplex cognitive radio network with nonlinear energy harvesting. IEEE Trans Green Commun Netw 2020;4(2):448–60.
[13] Koc A, Altunbas I, Basar E. Two-way full-duplex spatial modulation systems with wireless powered AF relaying. IEEE Wirel Commun Lett 2018;7(3):444–7.
[14] Deng P, Wang B, Wu W, Guo T. Transmitter design in MISO-NOMA system with wireless-power supply. IEEE Commun Lett 2018;22(4):844–7.
[15] Karami MA, Inman DJ. Linear and nonlinear energy harvesters for powering pacemakers from heart beat vibrations. In: Active and passive smart structures and integrated systems 2011, Vol. 7977. International Society for Optics and Photonics; 2011, 797703.
[16] Wei Z, Sun S, Zhu X, Kim DI, Ng DWK. Resource allocation for wireless-powered full-duplex relaying systems with nonlinear energy harvesting efficiency. IEEE Trans Veh Technol 2019;68(12):12079–93.
[17] Gu F, Niu J, Jiang L, Liu X, Atiquzzaman M. Survey of the low power wide area network technologies. J Netw Comput Appl 2020;149:102459.
[18] Raza U, Kulkarni P, Sooriyabandara M. Low power wide area networks: An overview. IEEE Commun Surv Tutor 2017;19(2):855–73.
[19] Bharadia D, McMilin E, Katti S. Full duplex radios. ACM SIGCOMM Comput Commun Rev 2013;43(4):375–86.
[20] Bembe M, Abu-Mahfouz A, Masonta M, Ngqondi T. A survey on low-power wide area networks for IoT applications. Telecommun Syst 2019;71(2):249–74.
[21] Georgiou O, Raza U. Low power wide area network analysis: Can LoRa scale? IEEE Wirel Commun Lett 2017;6(2):162–5.
[22] Centenaro M, Vangelista L. Time-power multiplexing for LoRa-based IoT networks: An effective way to boost LoRaWAN network capacity. Int J Wirel Inf Netw 2019;26(4):308–18.
[23] Finnegan J, Brown S. An analysis of the energy consumption of LPWA-based IoT devices. In: 2018 international symposium on networks, computers and communications (ISNCC). IEEE; 2018, p. 1–6.
[24] Parri L, Parrino S, Peruzzi G, Pozzebon A. Low power wide area networks (LPWAN) at Sea: Performance analysis of offshore data transmission by means of LoRaWAN connectivity for marine monitoring applications. Sensors 2019;19(14):3239.
[25] You CS, Yeom JS, Jung BC. Performance analysis of cooperative low-power wide-area network for energy-efficient B5G systems. Electronics 2020;9(4):680.
[26] Peruzzi G, Pozzebon A. A review of energy harvesting techniques for low power wide area networks (LPWANs). Energies 2020;13(13):3433.
[27] Sanislav T, Mois GD, Zeadally S, Folea SC. Energy harvesting techniques for internet of things (IoT). IEEE Access 2021;9:39530–49.
[28] Elahi H, Munir K, Eugeni M, Atek S, Gaudenzi P. Energy harvesting towards self-powered IoT devices. Energies 2020;13(21):5528.
[29] Sanislav T, Zeadally S, Mois GD, Folea SC. Wireless energy harvesting: Empirical results and practical considerations for Internet of Things. J Netw Comput Appl 2018;121:149–58.
[30] Kamalinejad P, Mahapatra C, Sheng Z, Mirabbasi S, Leung VC, Guan YL. Wireless energy harvesting for the Internet of Things. IEEE Commun Mag 2015;53(6):102–8.
[31] Perera TDP, Jayakody DNK. Analysis of time-switching and power-splitting protocols in wireless-powered cooperative communication system. Phys Commun 2018;31:141–51.
[32] Zhou X, Zhang R, Ho CK. Wireless information and power transfer: Architecture design and rate-energy tradeoff. IEEE Trans Commun 2013;61(11):4754–67.
[33] Jeffrey A, Zwillinger D. Table of integrals, series, and products. Academic Press; 2007.
[34] Yılmaz A, Kucur O. Performance of transmit antenna selection and maximal-ratio combining in dual hop amplify-and-forward relay network over Nakagami-m fading channels. Wirel Pers Commun 2012;67(3):485–503.
[35] Goldsmith A. Wireless communications. Cambridge university press; 2005.
[36] Abramowitz M, Stegun IA. Handbook of mathematical functions with formulas, graphs, and mathematical tables, Vol. 9. New York: Dover; 1972.
[37] Wang X. A study of harvested power and energy harvesting efficiency using frequency response analyses of power variables. Mech Syst Signal Process 2019;133:106277.
[38] Nguyen N-P, Ngo HQ, Duong TQ, Tuan HD, da Costa DB. Full-duplex cyber-weapon with massive arrays. IEEE Trans Commun 2017;65(12):5544–58.
[39] Nasir AA, Zhou X, Durrani S, Kennedy RA. Relaying protocols for wireless energy harvesting and information processing. IEEE Trans Wireless Commun 2013;12(7):3622–36.
[40] Yan Z, Chen S, Zhang X, Liu HL. Outage performance analysis of wireless energy harvesting relay-assisted random underlay cognitive networks. IEEE Internet Things J 2018;5(4):2691–9.